Analytica Chimica Acta 811 (2014) 60–69

Contents lists available at ScienceDirect

Analytica Chimica Acta

journal homepage: www.elsevier.com/locate/aca

Achieving second order advantage with multi-way partial least squares and residual bi-linearization with total synchronous fluorescence data of monohydroxy–polycyclic aromatic hydrocarbons in urine samples

Korina Calimag-Williams[a], Gaston Knobel[a], H.C. Goicoechea[b], A.D. Campiglia[a,*]

[a] Department of Chemistry, University of Central Florida, Orlando, FL 32816, USA
[b] Catedra de Quimica Analitica I, Facultad de Bioquimica y Ciencias Biologicas, Universidad Nacional del Litoral, Ciudad Universitaria, CC 242-S30001 Santa Fe, Argentina

HIGHLIGHTS

- Chemometrics of urine metabolites with total synchronous fluorescence data.
- Second-order advantage is obtained either with U-PLS/RBL or N-PLS/RBL.
- Five PAH metabolites are determined in the presence of strong spectral interference.

GRAPHICAL ABSTRACT

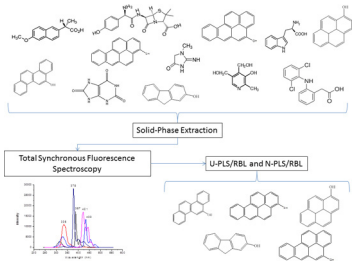

ARTICLE INFO

Article history:
Received 5 September 2013
Received in revised form 2 December 2013
Accepted 3 December 2013
Available online 11 December 2013

Keywords:
Polycyclic Aromatic hydrocarbons
Metabolites
Urine
Total synchronous fluorescence spectroscopy
Chemometrics

ABSTRACT

An attractive approach to handle matrix interference in samples of unknown composition is to generate second- or higher-order data formats and process them with appropriate chemometric algorithms. Several strategies exist to generate high-order data in fluorescence spectroscopy, including wavelength time matrices, excitation–emission matrices and time-resolved excitation–emission matrices. This article tackles a different aspect of generating high-order fluorescence data as it focuses on total synchronous fluorescence spectroscopy. This approach refers to recording synchronous fluorescence spectra at various wavelength offsets. Analogous to the concept of an excitation–emission data format, total synchronous data arrays fit into the category of second-order data. The main difference between them is the non-bilinear behavior of synchronous fluorescence data. Synchronous spectral profiles change with the wavelength offset used for sample excitation. The work presented here reports the first application of total synchronous fluorescence spectroscopy to the analysis of monohydroxy-polycyclic aromatic hydrocarbons in urine samples of unknown composition. Matrix interference is appropriately handled by processing the data either with unfolded-partial least squares and multi-way partial least squares, both followed by residual bi-linearization.

1. Introduction

The main motivation for using multivariate calibration algorithms in analytical chemistry results from their ability to extract information from complex samples without the need of previous chromatographic separation. Depending on the structure of the

* Corresponding author. Tel.: +1 407 823 4162; fax: +1 407 823 2252.
E-mail address: Andres.campiglia@ucf.edu (A.D. Campiglia).

0003-2670/$ – see front matter © 2013 Elsevier B.V. All rights reserved.
http://dx.doi.org/10.1016/j.aca.2013.12.004

data format, chemometric algorithms fall into first (vector), second (matrix), third (cube) or higher-order methods. The progression of orders partially reflects the ability of the algorithm to handle and obtain reliable data from matrixes of increasing complexity. Calibration methods that process first order data – first order algorithms – carry with them the first-order advantage, i.e. the ability to identify targeted species in the presence of sample concomitants with potential interference. In order to provide accurate quantitative information, first-order calibration methods require the laborious preparation of extensive calibration data sets with all the potential interference [1].

A more attractive approach to handle matrix interference is to generate second- or higher-order data formats and process them with appropriate algorithms. The second order advantage refers to calibration methods capable to provide accurate quantitation of targeted species in the presence of un-calibrated interference [2]. The application of second-order calibration methods requires second-order or tri-linear data, i.e. data describing each targeted species with a triad of invariant pure profiles. These include parallel factor analysis (PARAFAC) and multivariate curve resolution-alternating least-squares (MCR-ALS); as well as unfolded-partial least squares and multi-way partial least squares, both followed by residual bi-linearization (U-PLS/RBL and N-PLS/RBL) [1].

Several strategies exist to generate high-order data. Research in our lab has focused on the multidimensionality of fluorescence and/or phosphorescence spectroscopy. We have successfully combined wavelength-time matrices (WTMs) and time-resolved excitation–emission matrices (TREEMs) to second-order algorithms for the direct determination of polycyclic aromatic compounds [3–5] and some of their metabolites [6,7] in complex sample matrixes. WTMs consist of series of emission spectra recorded at different time delays from the laser excitation pulse. TREEMs are basically series of excitation–emission matrices recorded at different delay and gate times from the laser excitation pulse. In the case of a TREEM, the complete data set consists of emission intensity as a function of excitation wavelength, emission wavelength, and delay and gate times after the short duration of the excitation pulse. All emission intensity values can be assembled into a $J \times K \times L$ array, where J is the number of emission wavelengths, K is the number of excitation wavelengths and L is the number of time data points. A four-data array ($I \times J \times K \times L$) can then be obtained by adding the number of samples (I) to the $J \times K \times L$ array.

This article tackles a different aspect of generating high-order fluorescence data as it focuses on total synchronous fluorescence spectroscopy (TSFS). Synchronous fluorescence spectroscopy (SFS) refers to the simultaneous scanning of both the excitation (λ_0) and the emission (λ) monochromators while keeping a constant wavelength interval ($\Delta\lambda = \lambda - \lambda_0$) between them [8,9]. Synchronous fluorescence spectra recorded at a single $\Delta\lambda$ fit into the category of first-order data. Synchronous fluorescence spectra recorded at various $\Delta\lambda$s provide a data array with comprehensive information on the total synchronous fluorescence of the sample. Analogous to the concept of an EEM data format, TSF data arrays fit into the category of second-order data. The main difference between them is the non-bilinear behavior of TSF data. Synchronous fluorescence spectral profiles change with the wavelength offset used for sample excitation.

Only one TSFS report exists on achieving the second order advantage with second order algorithms. It describes the analysis of doxorubicin in human plasma of unknown composition [10]. The work presented here reports the first application of TSFS to the analysis of monohydroxy-polycyclic aromatic hydrocarbons (OHPAH) in urine samples. Due to their short elimination lifetime from the human body, the quantitative determination of OHPAH in urine samples provides valuable information on recent environmental exposure to polycyclic aromatic hydrocarbons (PAH). Biotransformation of PAH leads to the formation of multiple metabolites, some of which are prompt to participate in tumor initiation processes [9,11,12]. Previous articles on the SFS of OHPAH in urine samples base metabolites determination on synchronous spectral profiles recorded at single $\Delta\lambda$ values [13–16].

In this article, five OH-PAH – namely, 1-hydroxypyrene (1-OHPyr), 2-hydroxyfluorene (2-OHFlu), 3-hydroxybenzo[*a*]pyrene (3-OHB[*a*]P), 4-hydroxybenzo[*a*]pyrene (4-OHB[*a*]P) and 6-hydroxybenzo[*a*]pyrene (6-OHB[*a*]P) – are solid-phase extracted from urine samples on C18 silica cartridges and directly determined in the solvent extract (methanol) without previous chromatographic separation. The advantage of modeling TSFS data over the straightforward implementation of both synchronous fluorescence spectroscopy and first-derivative synchronous fluorescence spectroscopy is illustrated with the analysis of 6-OHChry and 4-OHB[*a*]P in the presence of relatively large concentrations of 1-OHPyr and 3-OHB[*a*]P, respectively. The presence of creatinine, naproxen, ibuprofen, diclofenac and amoxicillin in urine samples was investigated as potential interference in the analysis of OHPAH. We demonstrate that the combination of TSFS to either U-PLS/RBL or N-PLS/RBL provides robust screening approaches for the analysis of OHPAH in urine samples of unknown composition.

2. Theory

2.1. U-PLS/RBL

The first calibration step of this algorithm comprises concentration information only from standards; i.e. it excludes data from the unknown sample [17]. The I calibration data matrices $\mathbf{X}_{c,i}$ (size $J \times K$, where J and K are the number of channels in each dimension) are vectorized (unfolded) and used to calibrate a U-PLS model and the vector of calibration concentrations $\mathbf{y}$ ($N_c \times 1$, where N_c is the number of calibrated analytes). This step provides a set of loadings $\mathbf{P}$ and weight loadings $\mathbf{W}$ (both of size $JK \times A$, where A is the number of latent factors), as well as regression coefficients $\mathbf{v}$ (size $A \times 1$). The parameter A is obtained with the leave-one-out cross-validation technique [18]. If no unexpected interferences occur in the test sample, the analyte concentration is estimated via the following equation:

$$y_u = \mathbf{t}_u^T \mathbf{v} \tag{1}$$

where $\mathbf{t}_u$ is the test sample score, obtained by projection of the (unfolded) data for the test sample $\mathbf{X}_u$ onto the space of the A latent factors:

$$\mathbf{t}_u = (\mathbf{W}^T\mathbf{P})^{-1}\mathbf{W}^T \,\mathrm{vec}(\mathbf{X}_u) \tag{2}$$

When unexpected constituents occur in $\mathbf{X}_u$, the sample scores given by Eq. (2) are not suitable for analyte prediction with Eq. (1). The residuals of the U-PLS prediction step will be abnormally large in comparison with the typical instrumental noise. This situation can be handled by a separate procedure called residual bilinearization (RBL), which is based on singular value decomposition (SVD) modeling of interference effects. RBL aims at minimizing the norm of the residual vector $\mathbf{e}_u$, computed while fitting the sample data to the sum of the relevant contributions to the sample signal. For one interferent:

$$\mathrm{vec}(\mathbf{X}_u) = \mathbf{P}\,\mathbf{t}_u + \mathrm{vec}[g_{int}\,\mathbf{b}_{int}(\mathbf{c}_{int})^T] + \mathbf{e}_u \tag{3}$$

where $\mathbf{b}_{int}$ and $\mathbf{c}_{int}$ are the left and right eigenvectors of $\mathbf{E}_p$ (a $J \times K$ matrix containing the residual of the U-PLS prediction step) and g_{int} is a scaling factor:

$$(g_{int}, \mathbf{b}_{int}, \mathbf{c}_{int}) = \mathrm{SVD}_1(\mathbf{E}_p) \tag{4}$$

where SVD_1 indicates the process of taking only the first principal component.

During the RBL procedure, **P** is kept constant at the calibration values and $\mathbf{t}_u$ is varied until $||\mathbf{e}_u||$ is minimized. The minimization can be carried out using a Gauss-Newton procedure starting with $\mathbf{t}_u$ from Eq. (3). Once $||\mathbf{e}_u||$ is minimized in Eq. (3), the analyte concentrations are provided by Eq. (1), by introducing the final $\mathbf{t}_u$ vector found by the RBL procedure.

The number of unexpected constituents N_{unx} can be assessed by comparing the final residuals s_u with the instrumental noise level:

$$s_u = ||\mathbf{e}_u||/[JK - (N_c + N_{unx})]^{1/2} \quad (5)$$

where $\mathbf{e}_u$ is the same as the one in Eq. (3). The correct number of components is obtained from a plot of s_u versus the trial number of components. It will start at s_p – for a number of components equal to A – and show decreasing values until it stabilizes at a value compatible with the experimental noise.

2.2. N-PLS/RBL

Similar to U-PLS/RBL, N-PLS/RBL includes concentration information only in the calibration step. The I calibration data arrays and the vector of calibration concentrations **y** (size $I \times 1$) are combined to generate regression coefficients **v** (size $A \times 1$) and two sets of loadings, namely **W***j* and **W***k* of sizes $J \times A$ and $K \times A$. J and K refer to digitized wavelengths in emission and excitation, respectively [19]. A is the number of latent factors, which is usually selected by leave-one-out cross-validation technique. In the absence of unexpected components, the analyte concentration in the test sample is estimated with Eq. (1); where $\mathbf{t}_u$ is the test sample score vector obtained by appropriate projection of the test data onto the calibration loading matrices.

In order to handle the presence of unexpected constituents, residual bi-linearization resorts to the principal component analysis (PCA) of their contribution by minimizing the computed residuals while fitting the sample data to the sum of the relevant contributions. For N-PLS, the sum of contributions is given by Eq. (6):

$$\mathbf{X}_u = \text{reshape}\{\mathbf{t}_u[(\mathbf{W}_j| \otimes |\mathbf{W}_k)]\} + \mathbf{B}_{unx}\mathbf{G}_{unx}(\mathbf{C}_{unx})^T + \mathbf{E}_u \quad (6)$$

In this equation, "reshape" indicates transforming a $JK \times 1$ vector into a $J \times K$ matrix; matrices $\mathbf{B}_{unx}$, $\mathbf{G}_{unx}$ and $\mathbf{C}_{unx}$ are obtained by singular value decomposition of the error matrix $\mathbf{E}_p$ and $|\otimes|$ is the Kathri–Rao operator:

$$\mathbf{B}_{unx}\mathbf{G}_{unx}(\mathbf{C}_{unx})^T = SVD_1(\mathbf{E}_p) \quad (7)$$

During the RBL procedure, the loadings are kept constant at the calibration values, and $\mathbf{t}_u$ is varied until the final RBL residual error s_u is minimized using a Gauss–Newton procedure:

$$s_u = ||\mathbf{E}_u||/(JKI)^{1/2} \quad (8)$$

Analyte concentrations are then obtained by introducing the values of $\mathbf{t}_u$ vectors into Eq. (1).

3. Experimental

3.1. Chemicals

All solvents were Aldrich HPLC grade. All chemicals were analytical-reagent grade and utilized without further purification. Unless otherwise noted, Nanopure water was used throughout. 2-OHFlu, 1-OHPyr, 6-OHChry, creatinine, amoxicillin, diclofenac, ibuprofen and naproxen were purchased from Sigma-Aldrich. 3-OHB[*a*]P and 4-OHB[*a*]P were from Midwest Research Institute. All other chemicals were purchased from Fisher Chemical. The Sep-Pak C18 cartridges were purchased from Waters (Milford, MA). The synthetic urine solution was manufactured by RICCA Chemical Company (Arlington, TX) and purchased from Fischer Scientific. Its chemical composition mimicked main components of human urine at the concentrations found in healthy urine samples. Real human urine was collected randomly from healthy individual volunteers.

Note: Use extreme caution when handling OHPAH known to be extremely toxic.

3.2. Fluorescence measurements

Steady state excitation and fluorescence spectra and signal intensities were recorded with a commercial spectrofluorimeter (Photon Technology international). The excitation source was a continuous-wave 75 W pulsed xenon lamp with broadband illumination from 200 to 2000 nm. The excitation and emission monochromators had the same reciprocal linear dispersion (4 nm mm^{-1}) and accuracy (±1 nm with 0.25 nm resolution). The gratings were blazed at 300 and 400 nm, respectively. Detection was made with a photomultiplier tube with spectral response from 185 to 650 nm. The instrument was computer controlled using commercial software (Felix32) specifically designed for the system. Appropriate cut off filters were used to reject straight-light radiation and second-order emission. The collection of synchronous fluorescence spectra were carried out by pouring liquid samples into standard (1 × 1 cm) quarts cuvette. Otherwise noticed, fluorescence was collected at 90° angle from excitation using a wavelength off-set equal to 5 nm and an excitation/emission band-pass of 1 nm. All the spectra are uncorrected for instrumental response.

3.3. Preparation of stock solutions

Stock solutions of OHPAH were prepared by dissolving pure standards in methanol. Stock solutions of amoxicillin, diclofenac, ibuprofen and naproxen stock were prepared in methanol and kept in the dark at 4 °C until further use. Prior to dilution, stock solutions were monitored via room temperature fluorescence (RTF) spectroscopy for possible photo-degradation of metabolites. No changes on spectral profiles and fluorescence intensities were observed for a period of six months. Working solutions of OHPAH and pharmaceutical drugs were prepared daily by serial dilution with methanol.

3.4. Hydrolysis of urine samples

Urine samples were spiked with micro-litters of stock solutions of appropriate concentrations and equilibrated for 30 min to allow for the interaction of metabolites and naproxen with urine components such as urea and various salts. Then 500 μL of 0.1 M HCl was added to the sample and the mixture was buffered with 500 μL of 0.05 M potassium biphthalate sodium hydroxide buffer (pH 5.0). The buffered sample was shaken for 30 min at 1400 rpm to allow for urine hydrolysis.

3.5. Solid-phase extraction of urine samples

SPE was carried out with a Visiprep 12 port vacuum manifold (Supelco). Urine samples were processed through a Sep-Pak Plus SPE cartridge pre-conditioned with 10 mL of methanol and 10 mL of buffered water (pH = 5). The cartridges were sequentially washed with 10 mL of buffered water (pH = 5) and 5% methanol/water.

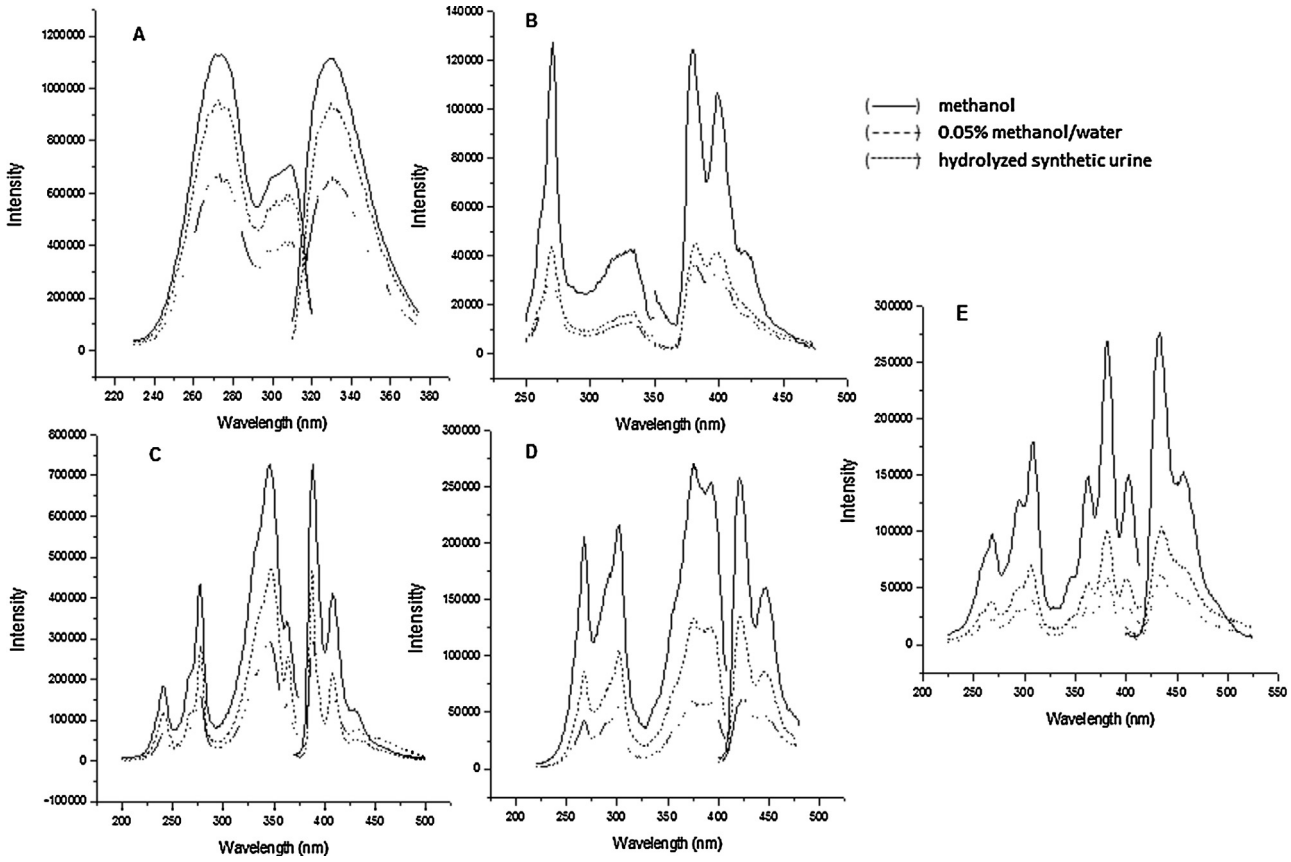

Fig. 1. Excitation and emission spectra of (A) 100 ng mL^{-1} 2OH-Flu, (B) 50 ng mL^{-1} 6OH-Chry, (C) 20 ng mL^{-1} 1OH-Pyr (D) 100 ng mL^{-1} 4OH-B[*a*]P, and 20 ng mL^{-1} 3OH-B[*a*]P in different media at excitation and emission band-pass = 2 nm/2 nm.

Without letting the cartridges to dry, OHPAH were eluted with 3 mL of pure methanol.

3.6. Preparation of calibration, validation and test sets

Calibration sets consisted of methanol solutions of pure metabolites at the following concentrations: 1-OHPyr (3, 5, 10, 15 and 25 ng mL^{-1}), 2-OHFlu (10, 25, 50, 75 and 100 ng mL^{-1}), 3-OHB[*a*]P (5, 10, 20, 30 and 50 ng mL^{-1}), 4-OHB[*a*]P (10, 25, 50, 75 and 100 ng mL^{-1}) and 6-OHChry (10, 25, 50, 75 and 100 ng mL^{-1}). Validation set #1 consisted of six synthetic mixtures (W-1–W-6) containing the five OHPAH in methanol-water (1% v/v) at final concentrations varying from 2 to 20 ng mL^{-1}. Validation set #2 included nine synthetic urine samples with (SUI) and without (SU) potential interference from pharmaceutical drugs. SU samples consisted of five synthetic urine samples (SU-1–SU-5) prepared with the five metabolites at final concentrations varying from 2 to 20 ng mL^{-1} and 0.5 μg mL^{-1} creatinine. The remaining four mixtures of validation set #2 (SUI-1–SUI-4) consisted of four synthetic urine samples containing the five OHPAH at 2 to 20 ng mL^{-1}, 0.5 μg mL^{-1} creatinine, naproxen, diclofenac, amoxicillin and ibuprofen. The final concentrations of the four pharmaceutical drugs varied from 10 ng mL^{-1} to 0.5 μg mL^{-1}. Validation set #3 consisted of nine real urine samples previously spiked with the five metabolites at 2 to 20 ng mL^{-1} final concentrations. Five of the real urine samples (RU-1–RU-5) contained no potential interference from creatinine and the four pharmaceutical drugs. The remaining four real urine samples (RUI-1–RUI-4) contained un-calibrated concentrations of creatinine, naproxen, diclofenac, amoxicillin and ibuprofen.

3.7. Software for chemometric analysis

All calculations were done using MATLAB 7.6 with the MVC2 graphical user interface and a user friendly MATLAB graphical interface written by Olivieri et al. [20].

4. Results and discussion

Early methods for the analysis of OHPAH in urine samples focused on 1-OHPyr [21,22]. Later methods expanded their scope to a larger number of metabolites, with particular attention to those resulting from exposure to EPA-PAH, i.e. PAH included in the Environmental Protection Agency (EPA) priority pollutants list [23]. Numerous HPLC and GC-MS methods currently exists for the analysis of EPA-PAH metabolites in urine samples, including 2-OHFlu, 1-OHPyr, 6-OHChry, 3-OHB[*a*]P and 4-OHB[*a*]P [24–29]. Reported methods often elute OHPAH from solid-phase extraction (SPE) cartridges with methanol. Pre-concentration is made via methanol evaporation prior to chromatographic determination. The SPE-TSFS procedure presented here consists of three simple steps, namely OHPAH extraction with C-18 cartridges, metabolites elution with methanol and TSFS determination without previous methanol evaporation.

4.1. Solid phase extraction of OHPAH

The efficiency of SPE was monitored via RTF spectroscopy, which required the previous knowledge of the fluorescence characteristics of OH-PAH in water, methanol and hydrolyzed urine. Fig. 1 illustrates the spectral features of the studied metabolites in the

Table 1
Room temperature fluorescence analytical figures of merit of OH-PAH in methanol/water, hydrolysed synthetic urine and methanol.

OH-PAH	$\lambda_{ex/em}$[a]	Methanol/water (0.05% v/v)				Hydrolyzed synthetic urine				Methanol			
		LDR[b]	R^2[c]	LOD[d]	LOQ[e]	LDR[b]	R^2[c]	LOD[d]	LOQ[e]	LDR[b]	R^2[c]	LOD[d]	LOQ[e]
2OH-Flu	267/328	1.60–50	0.999	0.48	1.58	1.47–50	0.999	0.44	1.47	1.33–50	0.999	0.40	1.33
6OH-Chry	273/381	0.90–50	0.995	0.27	0.90	0.90–50	0.995	0.26	0.87	0.60–50	0.996	0.18	0.60
1OH-Pyr	347/388	0.30–50	0.999	0.09	0.30	0.32–50	0.997	0.10	0.32	0.23–50	0.998	0.07	0.23
3OH-B[*a*]P	378/432	0.63–50	0.995	0.19	0.63	0.81–50	0.993	0.24	0.81	0.18–50	0.999	0.054	0.18
4OH-B[*a*]P	372/420	4.85–50	0.991	1.45	4.85	4.67–50	0.999	1.40	4.67	0.30–50	0.998	0.09	0.30

[a] Maximum excitation and emission wavelength in nm.
[b] Linear dynamic range in ng mL^{-1}.
[c] Correlation coefficient of calibration curve.
[d] Limit of detection (ng mL^{-1}) is calculated from 3 × standard deviation (s_b) of 16 blank measurements divided by slope (m) of the calibration curve.
[e] Limit of quantification (ng mL^{-1}) is calculated from $10S_b/m$.

three types of media. All spectra were recorded using the same excitation and emission band-pass (2 nm). No attempts were made to adjust slit widths to optimize spectra resolution, nor were the spectra corrected for instrumental response. The 2 nm band-pass provided satisfactory signal-to-background ratios (>3) for all the studied metabolites at the ng mL^{-1} concentration level. Although fluorescence intensities varied considerably with the liquid environment, the spectral profiles of the studied metabolites remained virtually the same in the three types of media. This fact provided a single set of maximum excitation (λ_{exc}) and emission (λ_{em}) wavelengths per metabolite. Table 1 summarizes the RTF analytical figures of merit (AFOM) of the studied metabolites in methanol/water 0.05% v/v, hydrolyzed synthetic urine, and pure methanol samples. The best linear fittings among the experimental data points were obtained via the least squares method [30]. The limits of detection (LOD) and the limits of quantitation (LOQ) were calculated from the standard deviation of 16 blank measurements (s_b) and the slope of the linear plot (m) according to $LOD = 3s_b/m$ and $LOQ = 10s_b/m$ [30].

The percentage of retention (%R) of the SPE procedure was calculated according to $\%R = (I_1 - I_2) \times 100$, where I_1 and I_2 refer to the fluorescence intensity of the metabolite before and after retention, respectively. The eluting efficiency (%E) was obtained from the equation $\%E = (m_E/m_R) \times 100$, where m_E and m_R refer to the eluted and retained mass of OHPAH, respectively. The mass of eluted metabolite was calculated multiplying the volume of eluted methanol (V_E) by the concentration of metabolite in the eluted solvent (C_E). The experimental values of the eluted concentrations were obtained from the calibration curves of the metabolites in methanol. The mass of retained metabolite was calculated from the product $V_S \times C_S \times (\%E)$, where V_S and C_S refer to the volume and concentration of the standard processed through the cartridge, respectively.

Table 2 summarizes the figures of merit of the SPE procedure obtained with 10 mL of sample and 3 mL of eluting solvent (methanol). Although larger sample volumes would provide larger pre-concentration factors, the 10 mL volume was enough to obtain satisfactory LODs at a relatively short analysis time. The volume of eluting solvent was optimized to achieve the best signal-to-background ratio without compromising OHPAH recoveries. Metabolites were spiked into the urine matrix 24 h prior to analysis. The spiked samples were submitted to acidic hydrolysis and then extracted via SPE. The percentages of overall recoveries (%OR) were calculated as the product of %R and %E, i.e. $\%OR = \%R \cdot \%E$. Within a confidence interval of 95% ($N = 3$), the overall recoveries in methanol–water standards and synthetic urine samples were the same. This agreement shows no matrix interference on the extraction of metabolites from synthetic urine samples.

4.2. Synchronous RTF Spectroscopy of OHPAH at single Δλ values

The best spectral resolution at single wavelength intervals was observed upon synchronous excitation with relatively small wavelength offsets. Δλ values smaller than 10 nm provided single fluorescence peaks for all the studied metabolites with narrow full-width at half maxima. The best compromise between spectral resolution and fluorescence intensity was obtained with Δλ values of 7 and 5 nm. The optimization of excitation/emission band-pass provided the best results with 2/2 nm (Δλ = 7 nm) and 1/1 nm (Δλ = 5 nm). The resulting spectra recorded from metabolite mixtures in methanol are shown in Fig. 2. Baseline resolution of the five metabolites was only achieved via first-derivative SFS. The main problem that confronts both SFS and the first derivative approach is illustrated in Fig. 3. The accurate determination of 6OH-Chry in the presence of relatively large concentrations of 1-OHPyr is no longer possible. The same is true for 4-OHB[*a*]P in the presence of relatively high concentrations of 3-OHB[*a*]P.

4.3. Total synchronous fluorescence spectroscopy combined to U-PLS/RBL or N-PLS/RBL

One possible solution for the analysis of OHPAH in matrixes of unknown composition consists in processing TSF data with second-order calibration methods. Although TSFS was recently combined to N-PLS, U-PLS and MCR-ALS for the analysis of PAH in water samples, the second-order advantage was not explored [31]. Calibration and validation sets were built with the five metabolites at toxicological relevant concentrations. Their values were adjusted to record synchronous profiles with and without significant contributions from other fluorescence concomitants and instrumental noise.

The five investigated concomitants included creatinine, naproxen, ibuprofen, diclofenac and amoxicillin. Creatinine is a metabolite usually present in human urine samples [32]. Naproxen, ibuprofen and diclofenac are well-known non-steroidal anti-inflammatory drugs [33,34] while amoxicillin is an antibiotic [35] of frequent use in our society. Comparison of their spectral features in Fig. 4 to those in Fig. 1 shows the strong spectral overlapping that exists with the five studied metabolites.

Their potential interference was tested at concentration levels usually found in human urine samples [32–35]. All measurements were made from solid-phase methanol extracts obtained as described previously. Synchronous fluorescence spectra were recorded from 200 to 550 nm, a wavelength interval that covered the entire excitation and emission range of the studied metabolites. Six wavelength intervals were used for synchronous excitation, namely 7, 41, 48, 54, 61and 108 nm. With the exception of Δλ = 7 nm – which provided the best resolution for the

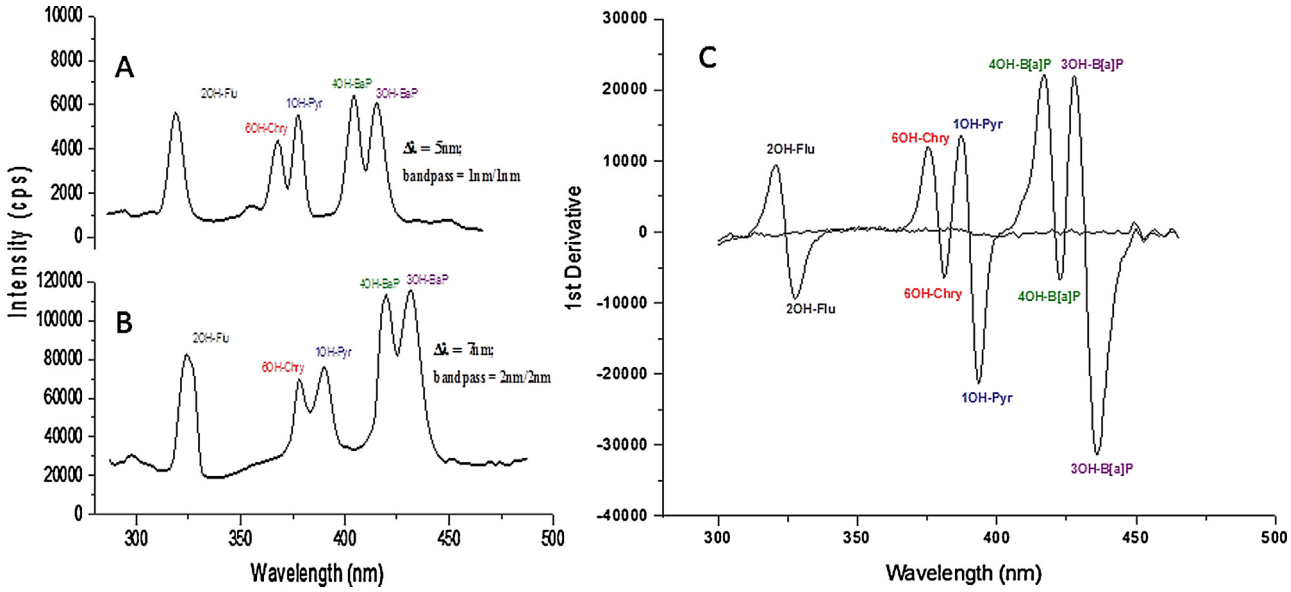

Fig. 2. Synchronous fluorescence spectra of OH–PAH mixture in methanol at $\Delta\lambda = 7$ nm: (A) excitation/emission band-pass = 1 nm/1 nm; (B) excitation/emission band-pass = 2 nm/2 nm; (C) first derivative of synchronous spectra of B. (A) and (B) mixture contains 10 ng mL^{-1} 3OH-B[*a*]P; 5 ng mL^{-1} 1OH-Pyr; 20 ng mL^{-1} 2OH-Flu; 20 ng mL^{-1} 4OH-B[*a*]P; 20 ng mL^{-1} 6OH-Chry.

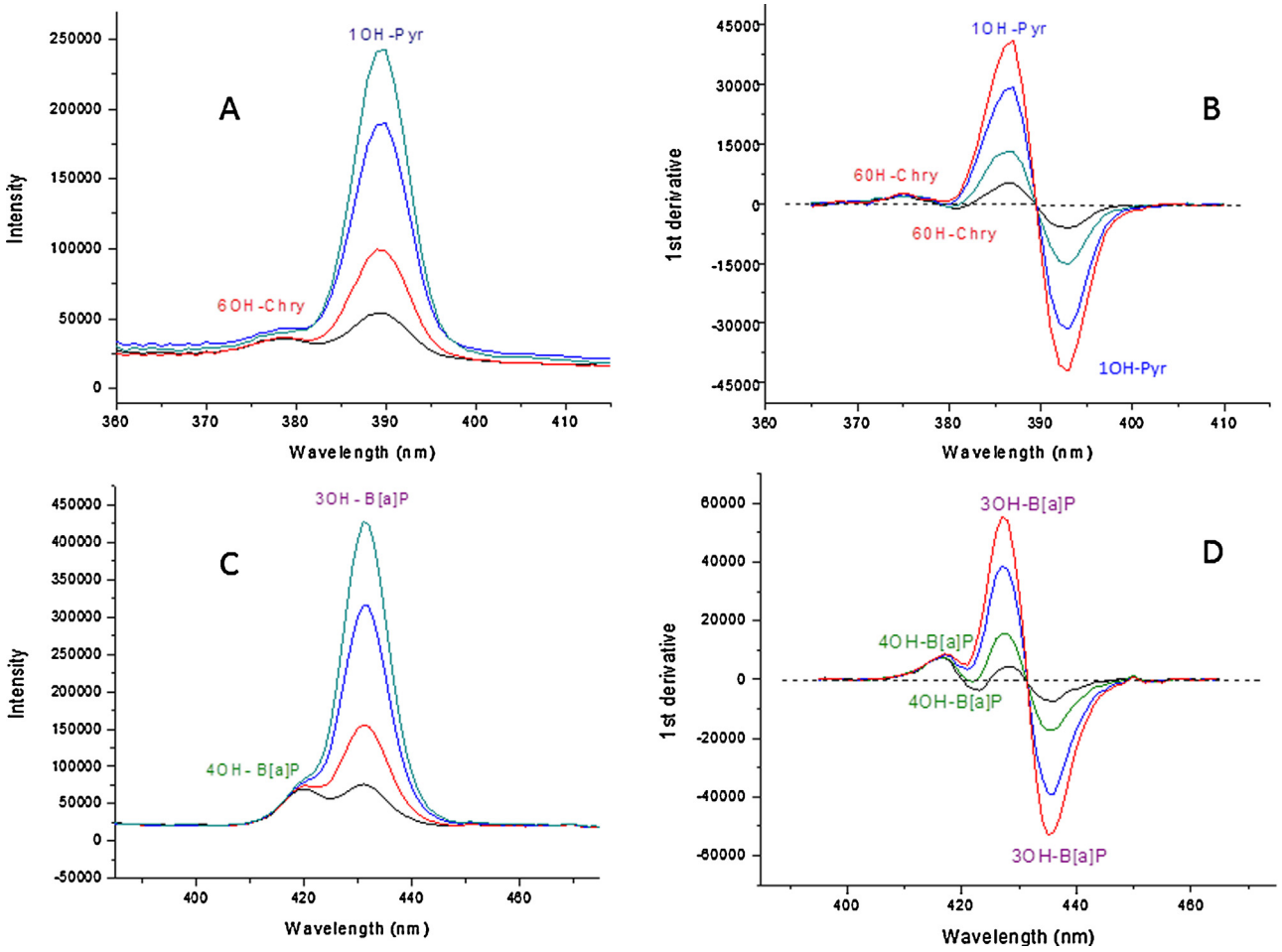

Fig. 3. Synchronous fluorescence spectra of binary mixtures of OHPAH in methanol recorded at $\Delta\lambda = 7$ nm and excitation/emission band-pass = 2 nm/2 nm: (A) 6OH-Chry and 1OH-Pyr mixture (B) first derivative of synchronous spectra of (A); (C) 4OH-B[*a*]P and 3OH-B[*a*]P mixture (D) first derivative of synchronous spectra of (C). Starting concentrations in (A) and (B) are 5 ng mL^{-1} 6OH-Chry and 5 ng mL^{-1} 1OH-Pyr, then increasing concentrations of 1OH-Pyr (10, 20 and 25 ng mL^{-1}). Starting concentrations in (C) and (D) are 10 ng mL^{-1} 4OH-B[*a*]P and 10 ng mL^{-1} 3OH-B[*a*]P, then increasing concentrations of 3OH-B[*a*]P (20,40 and 50 ng mL^{-1}).

Table 2
Figures of merit for the optimized SPE procedure in aqueous and urine samples.

OHPAH[a]	% Retention $R \pm S_R$[b]		% Elution Efficiency $E \pm S_E$[c]		% Overall Recovery OR $\pm S_{OR}$[d]		t_{exp}[e]
	H_2O/CH_3OH	Urine	H_2O/CH_3OH	Urine	H_2O/CH_3OH	Urine	
2OH-Flu	99.91 ± 0.10	99.79 ± 0.28	99.26 ± 1.78	95.74 ± 2.88	99.17 ± 1.79	95.53 ± 3.02	1.838
6OH-Chry	98.70 ± 0.65	98.85 ± 0.30	99.80 ± 1.40	100.0 ± 1.80	98.50 ± 1.11	98.85 ± 1.65	0.305
1OH-Pyr	99.29 ± 0.23	99.55 ± 0.38	89.10 ±1.32	88.51 ± 0.95	88.46 ± 1.49	88.11 ± 1.13	0.331
4OH-B[*a*]P	96.65 ± 0.24	94.18 ± 1.90	86.15 ± 1.38	89.0 ± 1.9 0	83.26 ± 1.12	83.82 ± 3.60	0.467
3OH-B[*a*]P	99.03 ± 0.32	99.63 ± 0.12	99.18 ± 1.44	99.80 ± 1.04	98.22 ± 1.48	99.43 ± 1.05	1.179

[a] The final concentrations of spiked samples are 50 ng mL^{-1} for, 2OH-Flu, and 6OH-Chry and 20 ng mL^{-1} for 1OH-Pyr, 3OH-B[*a*]P, and 4OH-B[*a*]P.
[b] R = % retention efficiency; S_R = standard deviation of R.
[c] E = % elution efficiency; S_E = standard deviation of E.
[d] OR = % overall recovery; S_{OR} = standard deviation of OR. S_{OR} values were based on three independent repetitions of the entire SPE procedure and were calculated according to the formula $S_{OR}/OR = [(S_R/\%R)^2 + (S_E/\%E)^2]^{1/2}$, where S_R and S_E are the standard deviations of $\%R$ and $\%E$, respectively.
[e] t_{exp} – t value calculated for experimental measurements according to Ref. [27]; $t_{critical} = 2.78$ ($\alpha = 0.05$; $N_1 = N_2 = 3$).

simultaneous determination of the six metabolites – the other wavelength intervals corresponded to the difference between the maximum emission and excitation wavelengths of 1-OHPyr (41 nm), 4-OHB[*a*]P (48 nm), 3-OHB[*a*]P (54 nm), 2-OHFlu (61 nm) and 6-OHChry (108 nm). Although each wavelength interval provided the most intense synchronous signal for its OHPAH, the accurate determination of each metabolite at its optimum wavelength interval was not possible due to strong spectral overlapping from the remaining compounds in the sample (see Fig. 5).

Table 3 summarizes the results obtained with the two algorithms. The statistical comparison of the results in Table 3 was made via the bivariate least-squares (BLS) regression method [36–38] and the elliptic joint confidence region (EJCR) test [39]. The plots of predicted versus actual concentrations provided the following slopes (b) and an intercepts (a): U-PLS/RBL, $b = 1.019 \pm 0.040$ and $a = -0.17 \pm 1.00$; N-PLS/RBL, $b = 1.018 \pm 0.035$ and $a = -0.28 \pm 0.88$. The EJRC plots of the slopes and the intercepts are shown in Fig. 6A. The elliptical domains obtained with both algorithms contain the theoretically predicted value of the slope (1) and the intercept (0). Both algorithms showed good predicting capability in the absence of interference. This was expected due to the ability of PLS to resolve the loss of bi-linearity of TSFS data. The slightly better precision obtained with N-PLS/RBL could be attributed to the use of the cube structure.

Tables 4 and 5 display the results obtained with unknown interference in synthetic and real urine samples. Since the presence of unknown components turns the residuals from the modeling of test sample signals abnormally large when compared to typical levels of instrumental noise, the number of unexpected components in each validation set was estimated via the post-calibration RBL procedure. The loadings were kept constant at the calibration values and $\mathbf{t}_u$ was varied until the final RBL residual error was minimized with a Gauss–Newton procedure. The stabilization of the residuals around the instrumental noise ($\sim 8.2 \times 10^3$ counts per second) suggested two or three unexpected components in both synthetic and real urine samples. Metabolites concentrations were obtained by introducing the new values of $\mathbf{t}_u$ vectors into Eq. (1). The statistical comparison of results made via the BLS regression method and the EJCR test provided the following slopes (b) and an intercepts (a): U-PLS/RBL, $b = 0.942 \pm 0.093$ and

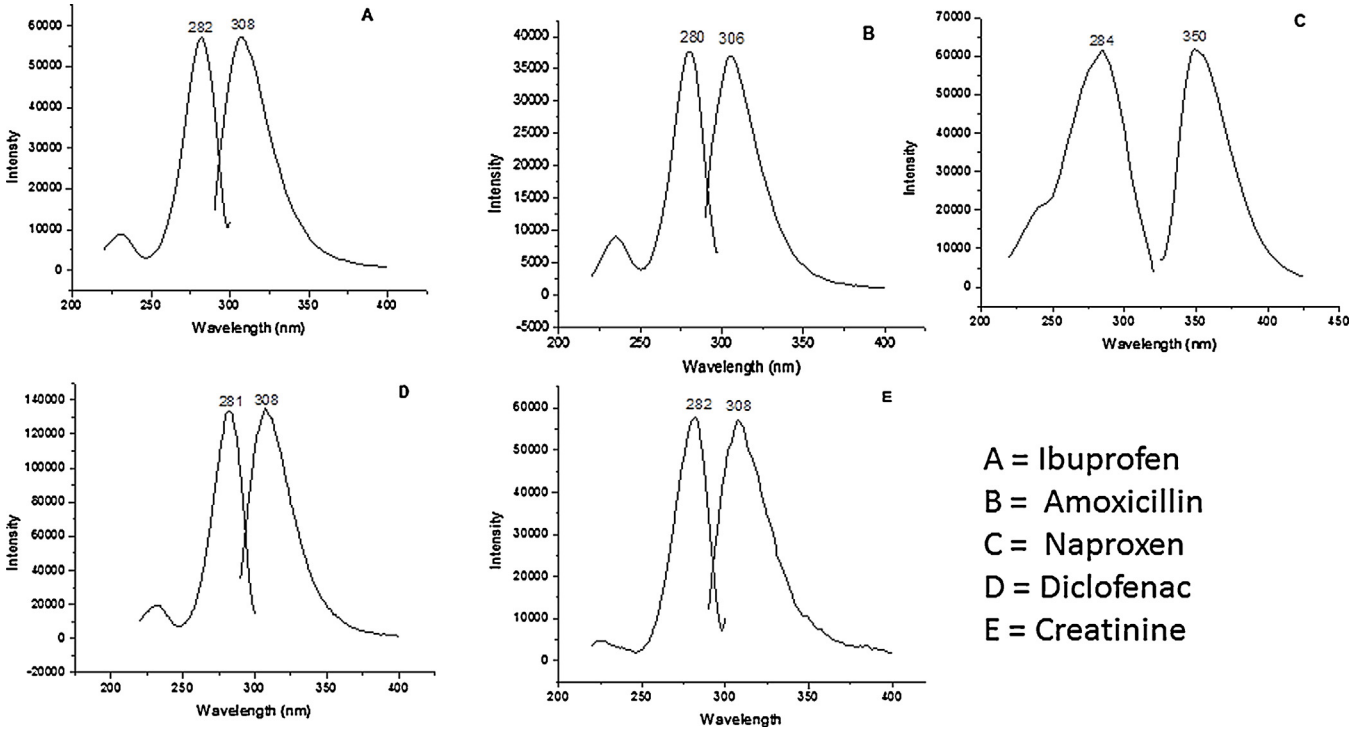

Fig. 4. Excitation and emission spectra of (A) 100 ng mL^{-1} ibuprofen, (B) 50 mg mL^{-1} amoxicillin, (C) 100 ng mL^{-1} naproxen, (D) 50 ng mL^{-1} diclofenac, (E) 50 mg mL^{-1} creatinine.

Table 3
U-PLS/RBL and N-PLS/RBL predictions on validation sets containing mixtures of five metabolites in water.

Sample	1OH-Pyr (ng mL^{-1})			2OH-Flu (ng mL^{-1})			3OH-B[*a*]P (ng mL^{-1})			4OH-B[*a*]P (ng mL^{-1})			6OH-Chry (ng mL^{-1})		
	Act.	U-PLS/RBL	N-PLS/RBL	Act.	U-PLS/RBL	N-PLS/RBL	Act.	U-PLS/RBL	N-PLS/RBL	Act.	U-PLS/RBL	N-PLS/RBL	Act.	U-PLS/RBL	N-PLS/RBL
W-1	2.0	2.1	2.0	6.7	7.0	7.0	10.0	10.7	11.0	13.3	14.0	13.7	21.7	21.8	21.8
W-2	2.7	2.6	2.6	13.3	13.0	13.0	6.7	6.1	6.4	10.0	9.6	9.6	10.0	9.7	9.7
W-3	5.0	4.7	4.7	16.7	16.3	16.2	3.3	2.9	2.9	8.3	8.0	8.1	18.3	17.8	18.0
W-4	6.7	6.8	6.9	20.0	20.8	21.0	10.0	10.3	10.3	11.7	12.1	12.0	11.7	11.1	11.2
W-5	8.3	8.0	8.0	8.3	8.0	8.0	6.7	6.0	6.0	21.7	21.1	21.2	13.3	13.0	13.1
W-6	3.3	3.5	3.5	11.7	12.2	12.3	3.3	3.7	3.6	8.3	8.8	8.7	8.3	8.7	8.7
Rec[a] (%)	–	100.0 (4.7)	99.7 (4.4)	–	100.8 (4.1)	101.2 (4.4)	–	98.2 (10.5)	99.1 (9.4)	–	100.6 (4.6)	99.9 (3.7)	–	98.7 (3.3)	99.0 (2.9)
REP[b] (%)	–	4.6	4.6	–	3.8	4.3	–	8.1	8.3	–	4.0	3.1	–	2.8	2.3

[a] Mean recovery. Values between parenthesis corresponds to standard deviation for $n = 6$.

[b] Relative error of prediction, $\mathrm{REP} = \frac{100}{\bar{c}}\left[\frac{1}{I}\sum_{1}^{I}(c_{\mathrm{act}} - c_{\mathrm{pred}})^2\right]^{1/2}$, where I is the number of samples, c_{act} and c_{pred} are the actual and predicted concentrations, and $\bar{c}$ is the mean concentration.

Table 4
U-PLS/RBL and N-PLS/RBL predictions on validation sets containing mixtures of five metabolites in synthetic urine samples with (SUI) and without (SUI) un-calibrated interference.

Sample	1OH-Pyr (ng mL^{-1})			2OH-Flu (ng mL^{-1})			3OH-B[*a*]P (ng mL^{-1})			4OH-B[*a*]P (ng mL^{-1})			6OH-Chry (ng mL^{-1})		
	Act.	U-PLS/RBL	N-PLS/RBL	Act.	U-PLS/RBL	N-PLS/RBL	Act.	U-PLS/RBL	N-PLS/RBL	Act.	U-PLS/RBL	N-PLS/RBL	Act.	U-PLS/RBL	N-PLS/RBL
SU-1	2.0	2.1	2.0	6.7	8.3	8.3	10.0	10.0	9.4	13.3	11.8	10.8	21.7	20.0	18.7
SU-2	2.7	3.0	2.9	13.3	15.4	12.4	6.7	5.4	5.3	10.0	7.7	7.7	10.0	9.6	9.2
SU-3	5.0	6.0	6.0	16.7	21.1	19.4	3.3	2.7	3.0	8.3	8.2	7.8	18.3	17.4	17.2
SU-4	6.7	6.9	6.9	20.0	21.4	19.7	10.0	11.2	10.9	11.7	10.2	10.3	11.7	11.7	11.8
SU-5	8.3	9.4	9.4	8.3	8.6	8.0	6.7	7.0	6.8	21.7	20.3	19.7	13.3	12.1	12.2
Mean (%)[a]	–	111.1 (6.2)	109.6 (7.1)	–	115.3 (10.1)	105.6 (13.6)	–	96.0 (13.8)	95.1 (11.2)	–	89.1 (7.9)	86.4 (6.9)	–	94.8 (3.7)	92.8 (5.3)
REP (%)[b]	–	13.6	13.5	–	18.2	11.4	–	11.3	10.8	–	11.6	14.4	–	6.9	10.4
SUI-1	2.0	1.9	2.2	6.7	6.6	5.5	10.0	8.3	9.3	13.3	12.1	11.8	21.7	18.3	19.2
SUI-2	2.7	2.9	2.8	13.3	12.2	11.1	6.7	9.4	8.1	10.0	7.7	7.6	10.0	10.1	10.2
SUI-3	5.0	4.4	5.2	16.7	10.9	18.4	3.3	2.9	2.6	8.3	8.2	8.2	18.3	16.6	16.1
SUI-4	6.7	4.7	6.2	20.0	10.6	18.9	10.0	10.9	10.2	11.7	10.6	10.6	11.7	10.1	11.9
Mean (%)[a]	–	90.2 (16.5)	103.0 (7.2)	–	77.2 (21.6)	92.6 (13.1)	–	105.3 (26.0)	98.5 (18.8)	–	89.1 (8.8)	88.5 (9.2)	–	90.6 (7.6)	95.0 (7.8)
REP(%)[b]	–	23.2	13.2	–	34.9	10.3	–	20.0	10.9	–	11.7	13.3	–	12.0	10.3

[a] Mean recovery. Values between parenthesis corresponds to standard deviation for $n = 5$.

[b] Relative error of prediction, $\mathrm{REP} = \frac{100}{\bar{c}}\left[\frac{1}{I}\sum_{1}^{I}(c_{\mathrm{act}} - c_{\mathrm{pred}})^2\right]^{1/2}$, where I is the number of samples, c_{act} and c_{pred} are the actual and predicted concentrations, and $\bar{c}$ is the mean concentration.

Table 5
U-PLS/RBL and N-PLS/RBL predictions on validation sets containing mixtures of five metabolites in real urine samples with (RUI) and without (RU) un-calibrated interference.

Sample	1OH-Pyr (ng mL^{-1})			2OH-Flu (ng mL^{-1})			3OH-B[*a*]P (ng mL^{-1})			4OH-B[*a*]P (ng mL^{-1})			6OH-Chry (ng mL^{-1})		
	Nom.	U-PLS/RBL	N-PLS/RBL	Nom.	U-PLS/RBL	N-PLS/RBL	Nom.	U-PLS/RBL	N-PLS/RBL	Nom.	U-PLS/RBL	N-PLS/RBL	Nom.	U-PLS/RBL	N-PLS/RBL
RU-1	2.0	1.9	2.1	6.7	6.6	6.5	10.0	10.4	10.1	13.3	15.7	15.4	21.7	19.9	20.3
RU -2	2.7	3.0	2.9	13.3	14.4	15.0	6.7	6.4	6.8	10.0	11.9	11.4	10.0	12.4	11.9
RU -3	5.0	4.3	4.2	16.7	14.7	15.2	3.3	5.0	4.7	8.3	10.0	6.7	18.3	17.0	17.1
RU -4	6.7	8.0	7.4	20.0	18.7	18.3	10.0	9.5	10.1	11.7	10.1	10.0	11.7	11.6	11.7
RU -5	8.3	6.7	8.0	8.3	9.4	9.7	6.7	7.0	6.8	21.7	20.3	19.5	13.3	11.0	12.5
Mean (%)[a]	–	98.8 (16.5)	100.6 (11.1)	–	100.4 (10.1)	101.9 (11.9)	–	110.3 (23.1)	109.4 (17.7)	–	107.4 (16.1)	97.0 (17.5)	–	98.0 (15.5)	99.8 (11.0)
REP (%)[b]	–	20.2	10.7	–	9.6	10.7	–	11.3	8.5	–	14.0	13.9	–	11.8	8.3
RUI-1		2.0	1.8	2.0	6.7	8.4	5.9	10.0	14.0	13.3	13.3	15.0	15.0	21.7	21.1
RUI-2		2.7	3.2	2.7	13.3	13.7	12.1	6.7	7.7	6.5	10.0	11.4	11.5	10.0	8.4
RUI-3		5.0	4.5	4.4	16.7	15.8	15.4	3.3	2.8	2.7	8.3	7.1	7.0	18.3	16.4
RUI-4		6.7	5.2	6.1	20.0	18.4	18.0	10.0	11.1	11.3	11.7	12.1	11.3	11.7	10.7
Mean (%)[a]	–	94.1 (17.5)	95.2 (5.7)	–	103.8 (15.2)	90.2 (1.7)	–	112.5 (22.9)	106.3 (21.9)	–	103.9 (13.2)	105.2 (14.2)	–	90.4 (5.6)	91.0 (3.5)
REP (%)[b]	–	18.3	9.3	–	8.0	9.8	–	25.6	21.6	–	10.5	14.1	–	8.2	8.3

[a] Mean recovery. Values between parenthesis corresponds to standard deviation for $n = 5$.

[b] Relative error of prediction, $\mathrm{REP} = \frac{100}{\bar{c}}\left[\frac{1}{I}\sum_{1}^{I}(c_{act} - c_{pred})^2\right]^{1/2}$, where I is the number of samples, c_{act} and c_{pred} are the actual and predicted concentrations, and $\bar{c}$ is the mean concentration.

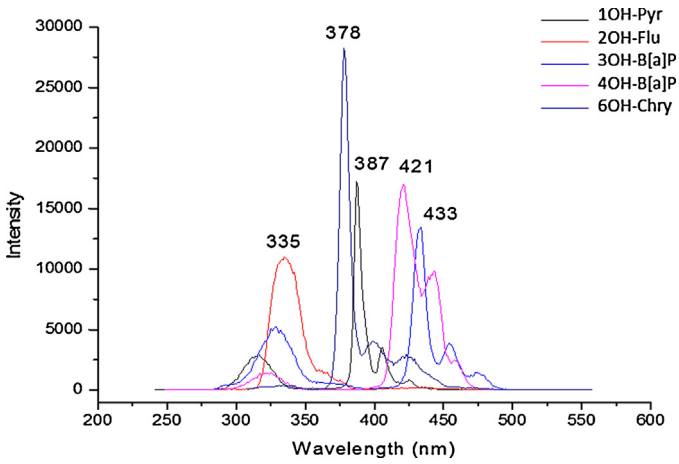

Fig. 5. Synchronous fluorescence spectra of OH-PAH recorded from individual methanol solutions of standards at different $\Delta\lambda$ offsets. All spectra were recorded using a 2 nm excitation and emission band-pass. Metabolite concentrations were as follows: 15 ng mL^{-1} 1OH-Pyr ($\Delta\lambda = 41$ nm); 50 ng mL^{-1} 2OH-Flu ($\Delta\lambda = 61$ nm); 10 ng mL^{-1} 3OH-B[*a*]P ($\Delta\lambda = 54$ nm); 25 ng mL^{-1} 4OH-B[*a*]P ($\Delta\lambda = 48$ nm) and 50 ng mL^{-1} 6OH-Chry ($\Delta\lambda = 108$ nm).

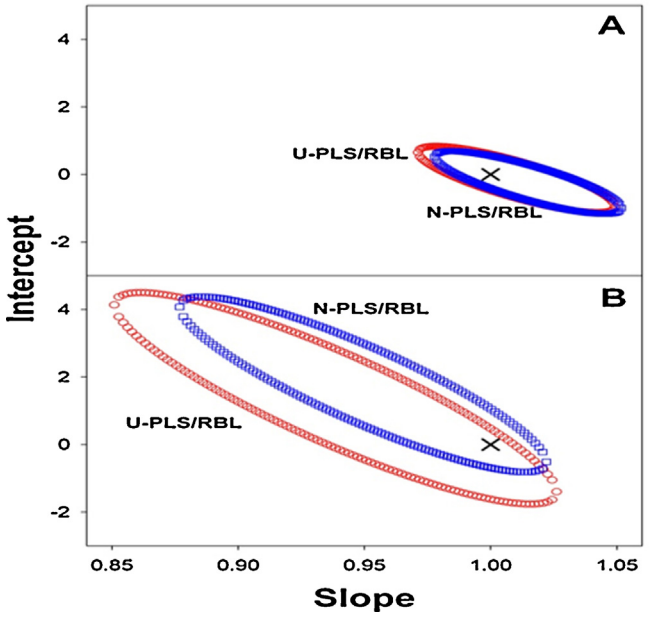

Fig. 6. Elliptic joint confidence regions plotting predicted versus actual concentrations of: (A) water samples summarized in Table 3; (B) synthetic urine and real urine samples summarized in Tables 4 and 5, respectively.

$a = 1.2 \pm 1.5$; N-PLS/RBL, $b = 0.949 \pm 0.067$ and $a = 1.8 \pm 1.7$. The EJRC plots of the slopes and the intercepts are shown in Fig. 6B. The elliptical domains obtained with both algorithms contain the theoretically predicted value of the slope (1) and the intercept (0). This fact rules out the possible presence of constant and proportional biases in the new method. Comparison of Table 3 to Tables 4 and 5 show better predictions in the absence of interference. This was expected due to the limited ability of RBL to modeling non-bilinear data.

4.4. Analytical figures of merit

Table 6 summarizes the analytical figures of merit of the six studied metabolites obtained by modeling TSFS data with

Table 6
Analytical figures of merit for the determination of OHPAH via TSFS/U-PLS/RBL and TSFS/N-PLS/RB.

	SEN (cps/mL ng^{-1})[a]		γ (mL ng^{-1})[b]		LOD (ng mL^{-1})[c]		LOQ (ng mL^{-1})[d]	
	U-PLS/RBL	N-PLS/RBL	U-PLS/RBL	N-PLS/RBL	U-PLS/RBL	N-PLS/RBL	U-PLS/RBL	N-PLS/RBL
1OH-Pyr	26,000	24,000	11.0	10.0	0.4	0.3	1.3	1.5
2OH-Flu	17,900	15,400	6.5	6.2	0.6	0.9	1.9	2.9
3OH-B[*a*]P	18,300	21,700	6.1	9.2	0.7	0.1	2.2	2.4
4OH-B[*a*]P	20,000	14,600	7.7	6.2	0.6	0.9	1.7	2.9
6OH-Chry	19,000	14,900	7.6	6.3	0.5	0.9	1.6	2.8

[a] cps = counts per second.
[b] Analytical sensitivity.
[c] LOD = limit of detection calculated considering 95% of probability [41].
[d] LOQ = limit of quantification calculated as LOD × (10/3.3) [41].

U-PLS/RBL and N-PLS/RBL. The sensitivity (SEN) was estimated according to the following expression [40]:

$$\mathrm{SEN}_{JAC} = \{\mathbf{v}^T[\mathbf{P}^T(\mathbf{I} - \mathbf{Z}_{\mathrm{int}}\mathbf{Z}_{\mathrm{int}}^{+})\mathbf{P}]^{-1}\mathbf{v}\}^{-1/2} \quad (9)$$

where the subscript *JAC* refers to the Jacobian approach, **P** is the matrix of calibration loadings, **v** is the vector of PLS regression coefficients in latent variable space, **I** is a unit matrix and $\mathbf{Z}_{\mathrm{int}}$ contains information regarding the interfering agents. The analytical sensitivity (γ), the limit detection (LOD) and the limit of quantitation (LOQ) were calculated according to Eqs. (10)–(12) [41]:

$$\gamma = \mathrm{SEN}/[var(x)]^{1/2} \quad (10)$$

$$\mathrm{LOD} = 3.3\,\mathrm{SD}(y_0) \quad (11)$$

$$\mathrm{LOQ} = 10\,\mathrm{SD}(y_0) \quad (12)$$

where var(x) is the instrumental uncertainty, the factor 3.3 corresponds to 5% for the so-called errors of type I and II, the factor 10 indicates 3.04 times the detection limit and SD(y_0) is the standard deviation for a blank sample containing low metabolites concentrations. These figures of merit demonstrate the potential of monitoring PAH metabolites at relevant toxicological levels.

5. Conclusion

The rigid and delocalized π electron system provides OHPAH with strong fluorescence for sensitive screening methodology. The main problem that comfronts the direct determination – no chromatogrphic separation – of metabolites via fluorescence spectroscopy is spectral overlapping. To some extent, spectral overlapping of OHPAH can be resolved with SFS and first-derivative SFS. Unfortunately, their specificity falls short for the analysis of metabolites with relatively large concentration differences. The good agreement among predicted and actual metabolite concentrations presented here demonstrate the ability of TSFS/U-PLS/RBL and TSFS/N-PLS/RBL to circumvent this problem. The two algorithms provided LODs varying between 0.3 ng mL^{-1} (1OH-Pyr) and 2.9 ng mL^{-1} (2OH-Flu and 4OH-B[*a*]P). These values, which place SPE-TSFS at the higher end of the reported chromatographic range [24–29], present ample opportunity for improvement since were obtained with only 10 mL of urine sample. The recovery values obtained via SPE-TSFS compare well to reported recoveries via GC-MS (≤80%) and HPLC (≤75%) [24–29]. Keeping in mind the ability of U-PLS/RBL and/or N-PLS/RBL to resolve spectral overlapping and the simplicity of the experimental procedure, the determination of OHPAH via SPE-TSFS appears to be a useful approach to monitor exposure of large populations to PAH contamination.

References

[1] G.M. Escandar, N.M. Faber, H.C. Goicoechea, A. Muñoz de la Peña, A.C. Olivieri, R.J. Poppi, Trends Anal. Chem. 26 (2007) 752–765.
[2] K.S. Booksh, B.R. Kowalski, Anal. Chem. 66 (1994) 782A–791A.
[3] H.C. Goicoechea, S. Yu, A.C. Olivieri, A.D. Campiglia, Anal. Chem. 77 (2005) 2608–2616.
[4] W.B. Wilson, E.C. Heider, F. Barbosa Jr., A.D. Campiglia, Curr. Top. Anal. Chem. 9 (2012) 1–23.
[5] H.C. Goicoechea, S. Yu, A.F.T. Moore, A.D. Campiglia, Talanta 101 (2012) 330–336.
[6] K. Vatsavai, H.C. Goicoechea, A.D. Campiglia, Anal. Biochem. 376 (2008) 213–220.
[7] H.C. Goicoechea, K. Calimag-Williams, A.D. Campiglia, Anal. Chim. Acta 717 (2012) 100–109.
[8] T. Vo-Dinh, Anal. Chem. 50 (1978) 396–401.
[9] J. Beyer, G. Jonsson, C. Porte, M.M. Krahn, F. Ariese, Environ. Toxicol. Pharmacol. 30 (2010) 224–244.
[10] A.V. Schenone, M.J. Culzoni, A.D. Campiglia, H.C. Goicoechea, Anal. Bioanal. Chem. 406 (2013) 8515–8523.
[11] A. Ramesh, S.A. Walker, D.B. Hood, M.D. Guillen, K. Schneider, E.H. Weyand, Int. J. Toxicol. 23 (2004) 301–333.
[12] F.J. Jongeneelen, R.P. Bos, R.B.M. Anzion, J.L.G. Theuws, P.T. Henderson, Scand. J. Work. Environ. Health 12 (1986) 137–143.
[13] A. Weston, E.D. Bowman, P. Carr, N. Rothman, P.T. Strickland, Carcinogenesis 14 (1993) 1053–1055.
[14] M.C. Poirier, A. Weston, B. Schoket, H. Shamkhani, C.F. Pan, M.A. Mc Diarmid, B.G. Scott, D.P. Deeter, J.M. Heller, D. Jacobson-Kram, N. Rothman, Polycyclic Aromat. Compd. 17 (1999) 197–208.
[15] M. Lamotte, R. Belfutmi, P. Fornier De Violet, P. Garrigues, M. Lafontaine, C. Dumas, Anal. Bioanal. Chem. 376 (2003) 816–821.
[16] H.-M. Yang, Y.-S. Wang, J.-H. Li, G.-R. Li, Y. Wang, X. Tan, J.-H. Xue, X.-L. Mao, R.-H. Kang, Anal. Chim. Acta 636 (2009) 51–57.
[17] S. Wold, P. Geladi, K. Esbensen, J. Øhman, J. Chemom. 1 (1987) 41–56.
[18] D.M. Haaland, E.V. Thomas, Anal. Chem. 60 (1988) 1193–1202.
[19] R. Bro, Multi-way analysis in the food industry, in: Doctoral Thesis, Netherlands, University of Amsterdam, 1998.
[20] A.C. Olivieri, W. Hai-Long, Y. Ru-Qin, Chemom. Intell. Lab. Syst. 96 (2009) 246.
[21] F.J. Jongeneelen, Int. Arch. Occup. Environ. Health 57 (1985) 47–55.
[22] F.J. Jongeneelen, Environ. Health 12 (1986) 137–143.
[23] U.S. Environmental Protection Agency, Methods for the determination of organic compounds in drinking water, in: EPA 600/4–88/039, U.S. Environmental Protection Agency, 1991.
[24] L. Kuusimaki, Y. Peltonen, P. Mutanen, K. Peltonen, K. Savela, Int. Arch. Occup. Environ. Health 77 (2004) 23–30.
[25] C.T. Kuo, H.W. Chen, J.L. Chen, J. Chromatogr. 805 (2004) 187–193.
[26] Y. Wang, W. Zhang, Y. Dong, R. Fan, G. Sheng, J. Fu, Anal. Bioanal. Chem. 383 (2005) 804–809.
[27] C.J. Smith, C.J. Walcott, W. Huang, V. Maggio, J. Grainger, D.G. Patterson Jr., J. Chromatogr. B 778 (2002) 157–164.
[28] B. Serdar, P.P. Egeghy, S. Waidyanatha, R. Gibson, S.M. Rappaport, Environ. Health Perspect. 111 (2003) 1760–1764.
[29] L.C. Romanoff, Z. Li, K.J. Young, N.C. Blakely, D.G. Patterson, C.D. Sandau, J. Chromatogr. B 835 (2006) 47–54.
[30] J.C. Miller, J.N. Miller, Statistics and Chemometrics for Analytical Chemistry, fourth ed., Prentice-Hall, Inc., New York, 2000.
[31] K. Kumar, A.K. Mishra, Anal. Methods 3 (2011) 2616–2624.
[32] A. Helander, C.A. Hagelberg, O. Beck, B. Petrini, Forensic Sci. Int. 189 (2009) e45–e47.
[33] J. Arancibia, A. Olivieri, G. Escandar, Anal. Bioanal. Chem. 374 (2002) 451–459.
[34] M. Winker, F. Tettenborn, D. Faika, H. Gulyas, R. Otterpohl, Water Res. 42 (2008) 3633–3640.
[35] D.P. Santos, M.F. Bergamini, M.V.B. Zanoni, Sens. Actuators, B 133 (2008) 398–403.
[36] A.C. Olivieri, J. Chemom. 19 (2005) 615–624.
[37] J.M. Lisý, A. Cholvadová, J. Kutej, Comput. Chem. 14 (1990) 189–192.
[38] J. Riu, F.X. Rius, J. Chemom. 9 (1995) 343–362.
[39] A.G. Gonzalez, M.A. Herrador, A.G. Asuero, Talanta 48 (1999) 729–736.
[40] F. Allegrini, A.C. Olivieri, Anal. Chem. 84 (2012) 10823–10830.
[41] A.C. Olivieri, N.M. Faber, J. Ferré, R. Boqué, J.H. Kalivas, H. Mark, Pure Appl. Chem. 78 (2006) 633–661.